

Multilayered metal core-shell nanostructures for inducing a large and tunable local optical field

Hongxing Xu*

*The Division of Solid State Physics, Lund University, Box 118, SE-22100, Sweden
and Institute of Physics, Chinese Academy of Science, Box 603, Beijing 100080, China*

(Received 2 May 2005; published 24 August 2005)

We examine the near-field optical properties of multilayered metal core-shell sphere nanostructures by extending the Mie theory, and demonstrate that the local-field enhancement can be increased by adding new metal shells. A local intensity enhancement of more than 10^5 times can be obtained in the cavity between the Ag core and the innermost Ag shell for proper configurations of multilayered Ag core-shell spheres. The high enhancement can be tuned from the red to the infrared region by varying the configurations of the core-shell nanostructures.

DOI: [10.1103/PhysRevB.72.073405](https://doi.org/10.1103/PhysRevB.72.073405)

PACS number(s): 78.67.Bf, 36.40.Vz, 42.25.Fx

The large field enhancement of metallic nanostructures is an intriguing phenomenon, which is a key feature of the surface-enhanced spectroscopy.¹⁻⁴ The metallic nanostructures for this purpose include mainly metal nanoparticles,^{1,2} metal nanoshells,⁵ metal nanorings,⁶ roughened metal surfaces,² and metal nanogratings.⁷ Amongst these, the metal nanoparticles have been most intensively studied. The large field enhancement of metal nanoparticle aggregates can allow single-molecule detection using surface-enhanced Raman scattering (SERS).⁴ The local intensity enhancement $M = |\mathbf{E}_{loc}/\mathbf{E}_0|^2$ in the interstitial sites of the aggregates can reach more than 10^5 times for a short interparticle separation down to 1 nm, while the electromagnetic part of the SERS enhancement factor $G \approx M^2$ can reach to 10^{10} times by taking into account both the illumination channel and the scattering channel.⁸

Metal nanoshells have also received a lot of attention recently.^{5,9-12} Most related studies were about the optical far field, such as absorption and extinction spectra. The tunable absorption from the visible to the infrared regions is extremely remarkable.^{5,9} Recent experiments have demonstrated that the wavelength selective absorption of metal nanoshells can be applied in cancer therapy.¹⁰ The local field enhancement of single metal nanoshells was also reported, but it is much weaker than the aggregates of metal nanoparticles.^{11,12}

In this paper, we investigate the optical near-field of multilayered metal core-shell sphere nanostructures. Although the optical far-field of the plasmon response of metal multi-shell nanostructures has been investigated,⁵ there is no obvious way to deduct the information of the local-field enhancement from such a study.¹³ For a single metal shell, the surface plasmon resonances (SPRs) of both the inner and outer surfaces can enhance the local field significantly inside the shell.¹⁴ The metal shell can be treated as an effective optical condenser. For a multilayered metal core-shell nanostructure, the large field enhancement can be obtained as the result of the collective coupling of surface plasmons of the metal core and the metal shells. A simple illustration is that the multilayered metal shells can act as a group of effective optical condensers to focus the incident light toward the geometric center multiplicatively. The intense focused light will then excite the surface plasmon of the metal core and induce an extremely large local-field enhancement in the cavity be-

tween the metal core and the innermost metal shell.

The model system is composed of a metal spherical core and a number of concentric metal spherical shells separated by dielectric materials (dielectric shells). The extended Mie theory is applied to calculate the intensity enhancement $M = |\mathbf{E}_{loc}/\mathbf{E}_0|^2$. By extending the Mie theory,¹⁵ the electromagnetic field in the core (denoted as the zeroth layer), the first layer to the S th layer and the surrounding medium [denoted as the $(S+1)$ th layer] of a multilayered core-shell sphere with S coating layers can be expressed as

$$\begin{aligned} \mathbf{E}_{loc} &= \sum_{n=1}^{\infty} \sum_{m=-n}^n [CN_{mn}(a_n^s N_{mn}^3 + c_n^s N_{mn}^1) \\ &\quad + CM_{mn}(b_n^s M_{mn}^3 + d_n^s M_{mn}^1)], \\ \mathbf{H}_{loc} &= \frac{k_s}{i\omega\mu_s} \sum_{n=1}^{\infty} \sum_{m=-n}^n [CN_{mn}(a_n^s M_{mn}^3 + c_n^s M_{mn}^1) \\ &\quad + CM_{mn}(b_n^s N_{mn}^3 + d_n^s N_{mn}^1)], \end{aligned} \quad (1)$$

where CM_{mn} and CN_{mn} are the expansion coefficients of the incident plane wave to the vector spherical harmonics M_{mn}^1 and N_{mn}^1 , and the superscript 1 and 3 represent the Bessel and Hankel forms, respectively. In principle, the scattering coefficients a_n^s, b_n^s , and the penetrating coefficients c_n^s, d_n^s of each layer can be obtained by the recurrence algorithms to solve the Maxwell boundary conditions.¹⁶⁻¹⁹ In order to avoid the tedious process of the recurrence algorithms, the scattering and penetrating coefficients are deduced directly here:

$$\begin{aligned} c_n^s &= \prod_{t=s}^S P_n^t, \\ d_n^s &= \prod_{t=s}^S Q_n^t, \\ a_n^s &= U_n^{s-1} c_n^s, \\ b_n^s &= V_n^{s-1} d_n^s, \end{aligned} \quad (2)$$

and the initial conditions $c_n^{S+1} = 1$ and $d_n^{S+1} = 1$. The set of U and V are defined as

$$U_n^{s<0} = 0, V_n^{s<0} = 0,$$

$$U_n^s = \frac{\kappa_s \psi_n(x_s) [\psi'_n(y_s) + U_n^{s-1} \xi'_n(y_s)] - \eta_s \psi'_n(x_s) [\psi_n(y_s) + U_n^{s-1} \xi_n(y_s)]}{\eta_s \xi'_n(x_s) [\psi_n(y_s) + U_n^{s-1} \xi_n(y_s)] - \kappa_s \xi_n(x_s) [\psi'_n(y_s) + U_n^{s-1} \xi'_n(y_s)]},$$

$$V_n^s = \frac{\eta_s \psi_n(x_s) [\psi'_n(y_s) + V_n^{s-1} \xi'_n(y_s)] - \kappa_s \psi'_n(x_s) [\psi_n(y_s) + V_n^{s-1} \xi_n(y_s)]}{\kappa_s \xi'_n(x_s) [\psi_n(y_s) + V_n^{s-1} \xi_n(y_s)] - \eta_s \xi_n(x_s) [\psi'_n(y_s) + V_n^{s-1} \xi'_n(y_s)]}, \quad (3)$$

and the set of P and Q are defined as

$$P_n^s = \frac{\psi_n(x_s) \xi'_n(x_s) - \psi'_n(x) \xi_n(x_s)}{\eta_s \xi'_n(x_s) [\psi_n(y_s) + U_n^{s-1} \xi_n(y_s)] - \kappa_s \xi_n(x_s) [\psi'_n(y_s) + U_n^{s-1} \xi'_n(y_s)]},$$

$$Q_n^s = \frac{\psi_n(x_s) \xi'_n(x_s) - \psi'_n(x) \xi_n(x_s)}{\kappa_s \xi'_n(x_s) [\psi_n(y_s) + V_n^{s-1} \xi_n(y_s)] - \eta_s \xi_n(x_s) [\psi'_n(y_s) + V_n^{s-1} \xi'_n(y_s)]}. \quad (4)$$

The Riccati-Bessel functions $\psi_n(z) = z j_n(z)$, $\xi_n(z) = z h_n^{(1)}(z)$, and $x_s = k_{s+1} r_s$, $y_s = k_s r_s$, $\kappa_s = k_{s+1}/k_s$, $\eta_s = \mu_{s+1}/\mu_s$, where k_s is the absolute value of the wave vector, μ_s is the magnetic permeability, and r_s is the radius of the outer surface of the sth layer.

Since electron-surface collisions in a thin metal shell dramatically shorten the electron mean-free path and cause an extra damping to the displacement of conducting electrons, the dielectric function of a thin metal shell should be modified from that of the bulk metal.⁹ To get the modified dielectric function, it is important to determine the electron mean-free path \bar{x} of electron-surface collisions precisely.²⁰

Figure 1 shows the local intensity enhancement factor M for different Ag core-shell spheres. The dielectric shells in Ag core-shell nanostructures have the same dielectric constant $n=1.45$. For convenience, the metal shells are denoted by subscripts of even numbers, while the dielectric shells by odd numbers. The host medium is a nonabsorbing material with a dielectric constant $n_h=1$. For a comparison, the spatial distribution of the local intensity enhancement M of a bare Ag sphere is shown in Fig. 1(a). The maximum $M=176$ at the resonant wavelength $\lambda=358$ nm. In Fig. 1(b), one Ag shell is added to the bare sphere in Fig. 1(a) with a separation to the metal core $d_1=2$ nm. The maximum enhancement $M=776$ in the cavity between the metal core and the metal shell at the favorite wavelength $\lambda=690$ nm. This maximum enhancement factor is about 4.5 times larger than for the bare Ag core in Fig. 1(a). In Fig. 1(c), one more metal shell is added to the core-shell particle in Fig. 1(b). The maximum enhancement $M=3.1 \times 10^3$, which is about four times more than in Fig. 1(b). With more Ag shells in Fig. 1(d) (three metal shells) and in Fig. 1(e) (four metal shells), the local intensity in the cavity between the metal core and the innermost metal shell is enhanced more and more. The maximum enhancement in Fig. 1(e) becomes $M=4 \times 10^4$, which is scaled as $\sim 4^4$ times more than the bare Ag sphere. This indicates that the multilayered metal shells do indeed act as a group of optical condensers to focus light multiplicatively, and the local intensity enhancement increases exponentially

with the power of the numbers of metal shells.

With even more additional shells, however, the increase of the enhancement can be reduced as the result of the increased absorption with the increase of the total metal thickness. For example, when a fifth metal shell (the thickness $d_{10}=8$ nm and the separation $d_9=75$ nm) is added to Fig. 1(e), a slightly higher enhancement $M=4.6 \times 10^4$ is obtained. But the increase is not as significant as the former additional metal shells. A sixth additional metal shell eventually decreases the enhancement below the value in Fig. 1(e).

A further enhancement can be obtained by optimizing the size of the core, the thicknesses of the metal shells and the separations between them. For $d_1=2$ nm, the optimized enhancement $M=6 \times 10^4$ for a four-Ag-shell core-shell sphere. However, the more efficient way is to reduce d_1 to increase the surface plasmon coupling of the metal core and the innermost metal shell, where $M \sim 1/d_1^2$ in the cavity. In Fig. 1(f), d_1 is reduced to 1 nm from Fig. 1(e), and a much higher enhancement is obtained. The maximum enhancement $M=1.2 \times 10^5$. Such a high enhancement is caused by the redistribution of the electromagnetic field focused by metal shells multiplicatively to a very small region. To average over the whole enhancement in Fig. 1(f), the mean enhancement is about 88 times, which is quite comparable to the enhancement of single-component metal particles.

It should be also noted that such a high enhancement is not a singularity for a certain core-shell sphere nanostructure. A similar enhancement over 10^5 times for $d_1=1$ nm can be easily obtained by varying the thicknesses (2–10 nm) of metal shells and the separations (10–100 nm) between them. Usually, too thin or too thick metal shells do not benefit the field enhancement. For thin metal shells, the damping due to electron-surface collisions broadens the SPR peak and decreases the field enhancement. For thick metal shells, however, the large absorption also diminishes the field enhancement. Too large separations between metal shells, which decouple their SPRs, do not benefit the enhancement either.

For metal nanoparticle aggregates, such a high enhancement over 10^5 times is also possible at the same interparticle

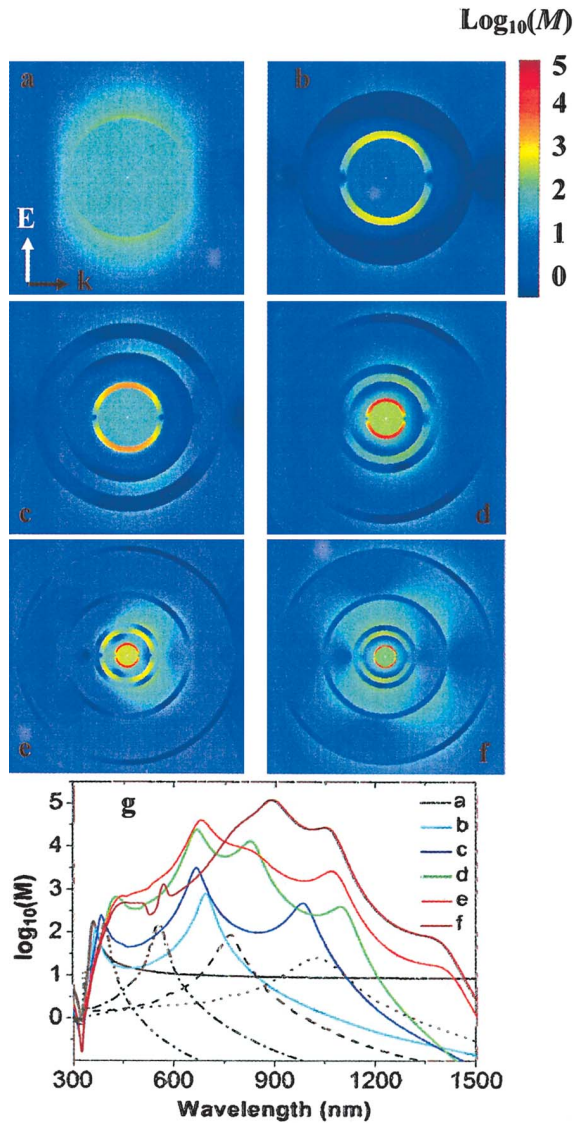


FIG. 1. (Color) Spatial distribution of the local intensity enhancement M in a logarithmic scale (colored) in the plane through the symmetrical center of the core-shell sphere nanostructures and parallel to the incident polarization \mathbf{E} and the wave vector \mathbf{k} for (a) a bare Ag sphere, (b) the same core but with one Ag shell, (c) with an additional Ag shell enclosing the core-shell nanostructure of (b), (d) with a third Ag shell enclosing the core-shell nanostructure of (c), (e) with a fourth Ag shell enclosing the core-shell nanostructure of (d). The radius $r_0=10$ nm. The thicknesses of the Ag shells are $d_2=10$ nm, $d_4=5$ nm, $d_6=5$ nm and $d_8=5$ nm for the first to the fourth Ag shell respectively. The corresponding separations between the core and the innermost Ag shell and the neighboring shells are $d_1=2$ nm, $d_3=5$ nm, $d_5=25$ nm, and $d_7=40$ nm, respectively. (f) shows the case same as (e) but with $d_1=1$ nm. The incident wavelength λ for (a)–(f) is 358, 690, 664, 665, 678, and 888 nm, respectively. (g) M at the point $rd=0.25$ nm away from the surface of the Ag core along the direction of the incident polarization versus the incident wavelength for (a)–(f) (the solid lines). The discrete lines show M at the same point for the outermost Ag shells only of (b)–(e) from the left to the right, respectively. The filled dielectric medium is the same.

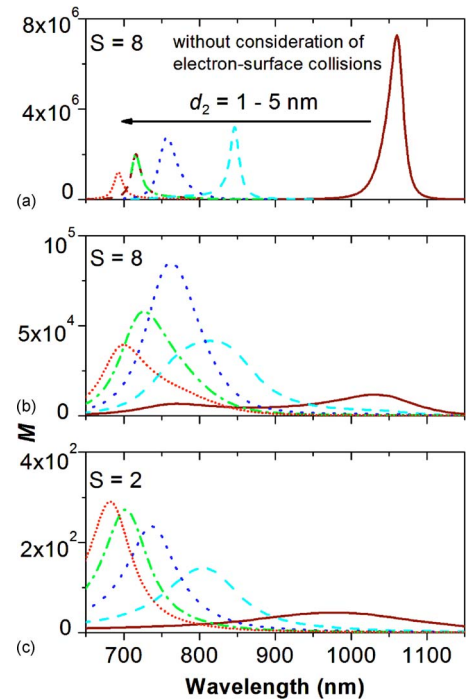


FIG. 2. (Color online) The local intensity enhancement M vs the incident wavelength λ for a four-Ag-shell sphere nanostructure (a) without and (b) with the consideration of electron-surface collisions, (c) a single-Ag-shell sphere with the consideration of electron-surface collisions. The thickness of the first Ag shell varies as $d_2=1, 2, 3, 4, 5$ nm the Ag core $r_0=5$ nm, and the separation $d_1=1$ nm for all the cases. In (a) and (b), the other separations $d_3=20$ nm, $d_5=25$ nm, $d_7=40$ nm, and the thicknesses of the other Ag shells $d_4=3$ nm, $d_6=3$ nm, $d_8=4$ nm.

separation $d=1$ nm.⁸ But the pointlike “hot” volumes in the interstices of aggregates are much smaller than in metal core-shell nanostructures. In Fig. 1(f), the hot volume includes almost the whole cavity between the metal core and the innermost metal shell, except for the smaller equator part which is perpendicular to the incident polarization. Therefore for a similar enhancement factor, the multilayered metal core-shell nanostructures can supply larger hot volumes than the metal nanoparticle aggregates. Moreover, the local-field enhancement in metal core-shell spheres are independent of the incident polarization due to the high spherical symmetries, while a strong polarization dependency was observed in the metal nanoparticle aggregates.^{21,22}

As indicated in Fig. 1(g), the SPR couplings of the metal core and the metal shells are very complex. There is no exact analytical solution to obtain the field enhancement. The resonance peaks of the metal core-shell spheres (the colored lines) are not simply overlaps of the single metal core (the black solid line) and the single metal shells (the discrete lines), but with new peaks due to the strong core-shell and shell-shell interactions. Some general rules, however, may be still helpful to obtain the high enhancement. For example, in order to maintain a high enhancement obtained in a certain configuration of core-shell nanostructure, the increase of the thickness of a metal shell which results in a *blueshift* of the SPR usually needs a compensation of the increase of the shell radius which results in a *redshift* of the SPR, and vice versa.

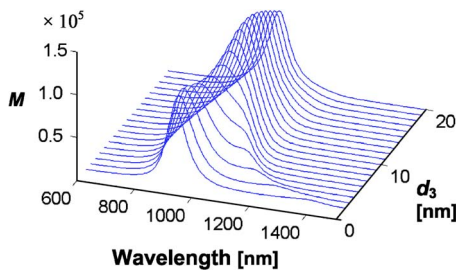


FIG. 3. (Color online) The local intensity enhancement M vs the incident wavelength λ for a four-Ag-shell sphere nanostructure with the separation d_3 between the two innermost Ag shells varying from 2 to 20 nm (increasing in steps of 1 nm). The radius of the Ag core $r_0=10$ nm. The other separations $d_1=1$ nm, $d_5=35$ nm, and $d_7=60$ nm. The thicknesses of the Ag shells $d_2=6$ nm, $d_4=3$ nm, $d_6=4$ nm, and $d_8=5$ nm.

For thin metal shells, it is known that electron-surface collisions can dramatically broaden and reduce the absorption peak.⁹ In the optical near field, such broadening effect to reduce the local field enhancement becomes even more dramatic. Figure 2 compares the cases with and without the consideration of electron-surface collisions. With the broadening effect, the overall peak enhancement in Fig. 2(b) will be about two orders less than without the broadening effect in Fig. 2(a). In the case a very thin metal shell $d_2=1$ nm, the strong broadening effect can reduce the peak enhancement more than three orders.

For the suitable separations between metal shells, the resonance wavelengths of multilayered metal core-shell spheres are mainly determined by the SPRs of the metal core and the innermost metal shell. Comparing Fig. 2(b) to the case of a single-Ag-shell core-shell sphere in Fig. 2(c), except for the enhancement factor, the resonance wavelength for the same d_2 in Fig. 2(b) is quite similar, except for a slight redshift which is caused by the retardation of the transmitted light through the metal shells. The peak wavelength can be tuned from the infrared to the red regions by increasing the thickness of the innermost metal shell d_2 from 1 nm to 5 nm.

When neighboring metal shells in a multilayered core-shell nanostructure are very close to each other, the resonant peak starts to split. Figure 3 shows such a case for a four-Ag-shell sphere with a varying separation between the first and the second Ag shell d_3 . When d_3 is less than ~ 7 nm, the splitting of the resonance peak is quite clear. A smaller separation d_3 causes a larger splitting. With the increase of d_3 , the split peaks gradually merge to a main peak. The splitting effect can be understood by the “hybridizations” of the SPRs of the neighboring metal shells, which results in the bonding and antibonding energy levels.⁵ For a larger separation, these two energy levels are degenerated. It is notable that the splitting diminishes the field enhancement, while the merging gives a higher enhancement which is attributed to both the bonding and the antibonding resonances.

Finally, the preceding results about the extremely large field enhancement and its tunability for multilayered metal core-shell nanostructures may imply the potential applications in single-molecule surface-enhanced spectroscopy. With the wavelength selective enhancement, multichannel detections can be possible. It would be more promising if multilayered metal core-shell nanoparticles substitutes single-layered metallodielectric core/shell nanoparticles for cancer therapy¹⁰ and for spectroscopic tags.²³

In summary, we have investigated the near-field optical properties of multilayered metal core-shell sphere nanostructures by extending the Mie theory. We show that the multilayered metal shells can act as a group of optical condensers to focus light multiplicatively. The extremely large local intensity enhancement over 10^5 times can be obtained in the cavity between the Ag core and the innermost Ag shell for proper configurations of multilayered core-shell spheres. The strong core-shell and shell-shell interactions determine the peak wavelengths and enhancement. The high enhancement can be tuned from the red to the infrared regions by varying the configurations of the core-shell nanostructures.

We acknowledge the Swedish Foundation for Strategic Research and the Swedish Natural Science Research Council.

*Fax: +86 10 82648013. Email: hongxingxu@aphy.iphy.ac.cn

¹G. C. Schatz and R. V. Duyne, in *Handbook of Vibrational Spectroscopy*, edited by J. M. Chalmers and P. R. Griffiths (Wiley & Sons, New York, 2002), p. 759.

²M. Moskovits, *Rev. Mod. Phys.* **57**, 783 (1985).

³J. R. Lakowicz, *Anal. Biochem.* **298**, 1 (2001).

⁴K. Kneipp *et al.*, *J. Phys.: Condens. Matter* **14**, R597 (2002).

⁵E. Prodan *et al.*, *Science* **302**, 419 (2003).

⁶J. Aizpurua *et al.*, *Phys. Rev. Lett.* **90**, 057401 (2003).

⁷F. J. GarciaVidal *et al.*, *Phys. Rev. Lett.* **77**, 1163 (1996).

⁸H. X. Xu *et al.*, *Phys. Rev. Lett.* **93**, 243002 (2004).

⁹R. D. Averitt *et al.*, *Phys. Rev. Lett.* **78**, 4217 (1997).

¹⁰D. P. O’Neal *et al.*, *Cancer Lett. (Shannon, Irel.)* **209**, 171 (2004).

¹¹S. J. Oldenburg *et al.*, *J. Chem. Phys.* **111**, 4729 (1999).

¹²M. Kerker and C. G. Blatchford, *Phys. Rev. B* **26**, 4052 (1982).

¹³M. Ohtsu, *Near-field Nano-optics* (Kluwer/Plenum, New York, 2004).

¹⁴J. Enderlein, *Appl. Phys. Lett.* **80**, 315 (2002).

¹⁵G. Mie, *Ann. Phys.* **25**, 377 (1908).

¹⁶R. Bhandari, *Appl. Opt.* **24**, 1960 (2004).

¹⁷J. Sinzig *et al.*, *Appl. Phys. A: Solids Surf.* **58**, 157 (1994).

¹⁸B. R. Johnson, *Appl. Opt.* **35**, 3286 (1996).

¹⁹D. D. Smith *et al.*, *J. Opt. Soc. Am. B* **19**, 2449 (2002).

²⁰The electron free path x of electron-surface collisions in a thin metal shell is either $x=r_b \cos \theta - \sqrt{r_a^2 - r_b^2} \sin^2 \theta$ ($\sin \theta \leq r_a/r_b$) connecting the inner surface and the outer surface of the shell, or $x=2r_b \cos \theta$ ($\sin \theta > r_a/r_b$) between two points on the outer surface but without cutting the inner surface, where θ is the angle between x and the radius (the cross point is the end of x on the outer surface), r_a and r_b are the radii of the inner and outer surfaces of the shell, respectively. Hence $\bar{x} = \int_0^{\pi/2} x \sin \theta d\theta$. \bar{x} is larger than the thickness of the shell as used in Ref. 9.

²¹K. A. Bosnick *et al.*, *J. Phys. Chem. B* **106**, 8096 (2002).

²²H. X. Xu and M. Käll, *ChemPhysChem* **4**, 1001 (2003).

²³W. E. Doering and S. Nie, *Anal. Chem.* **75**, 6171 (2003).